

¹ **Critical transitions and the fragmenting of global forests**

² **Leonardo A. Saravia^{1 3}, Santiago R. Doyle¹, Benjamin Bond-Lamberty²**

³ 1. Instituto de Ciencias, Universidad Nacional de General Sarmiento, J.M. Gutierrez 1159 (1613), Los
⁴ Polvorines, Buenos Aires, Argentina.

⁵ 2. Pacific Northwest National Laboratory, Joint Global Change Research Institute at the University of
⁶ Maryland–College Park, 5825 University Research Court #3500, College Park, MD 20740, USA

⁷ 3. Corresponding author e-mail: lsaravia@ungs.edu.ar

⁸ **keywords:** Forest fragmentation, early warning signals, percolation, power-laws, MODIS, critical transitions

⁹ **Running title:** Critical fragmentation in global forest

¹⁰ **Abstract**

¹¹ 1. Forests provide critical habitat for many species, essential ecosystem services, and are coupled to
¹² atmospheric dynamics through exchanges of energy, water and gases. One of the most important
¹³ changes produced in the biosphere is the replacement of forest areas with human dominated landscapes.
¹⁴ This usually leads to fragmentation, altering the sizes of patches, the structure and function of the
¹⁵ forest. Here we studied the distribution and dynamics of forest patch sizes at a global level, examining
¹⁶ signals of a critical transition from an unfragmented to a fragmented state.

¹⁷ 2. We used MODIS vegetation continuous field to estimate the forest patches at a global level and de-
¹⁸ fined wide regions of connected forest across continents and big islands. We search for critical phase
¹⁹ transitions, where the system state of the forest changes suddenly at a critical point in time; this
²⁰ implies an abrupt change in connectivity that causes an increased fragmentation level. We studied the
²¹ distribution of forest patch sizes and the dynamics of the largest patch over the last fourteen years,
²² as the conditions that indicate that a region is near a critical fragmentation threshold are related to
²³ patch size distribution and temporal fluctuations of the largest patch.

²⁴ 3. We found some evidence that allows us to analyze fragmentation as a critical transition: most regions
²⁵ followed a power-law distribution over the 14 years. We also found that the Philippines region probably
²⁶ went through a critical transition from a fragmented to an unfragmented state. Only the tropical forest
²⁷ of Africa and South America met the criteria to be near a critical fragmentation threshold.

28 4. This implies that human pressures and climate forcings might trigger undesired effects of fragmentation,
29 such as species loss and degradation of ecosystems services, in these regions. The simple criteria
30 proposed here could be used as an early warning to estimate the distance to a fragmentation threshold
31 in forest around the globe and a predictor of a planetary tipping point.

32 Introduction

33 Forests are one of the most important biomes on earth, providing habitat for a large proportion of species
34 and contributing extensively to global biodiversity (Crowther et al., 2015). In the previous century human
35 activities have influenced global bio-geochemical cycles (Bonan, 2008; Canfield, Glazer, & Falkowski, 2010),
36 with one of the most dramatic changes being the replacement of 40% of Earth's formerly biodiverse land
37 areas with landscapes that contain only a few species of crop plants, domestic animals and humans (J. A.
38 Foley et al., 2011). These local changes have accumulated over time and now constitute a global forcing
39 (Barnosky et al., 2012).

40 Another global scale forcing that is tied to habitat destruction is fragmentation, which is defined as the
41 division of a continuous habitat into separated portions that are smaller and more isolated. Fragmentation
42 produces multiple interwoven effects: reductions of biodiversity between 13% and 75%, decreasing forest
43 biomass, and changes in nutrient cycling (Haddad et al., 2015). The effects of fragmentation are not only
44 important from an ecological point of view but also that of human activities, as ecosystem services are deeply
45 influenced by the level of landscape fragmentation (Mitchell et al., 2015).

46 Ecosystems have complex interactions between species and present feedbacks at different levels of organiza-
47 tion (Gilman, Urban, Tewksbury, Gilchrist, & Holt, 2010), and external forcings can produce abrupt changes
48 from one state to another, called critical transitions (Scheffer et al., 2009). These abrupt state shifts cannot
49 be linearly forecasted from past changes, and are thus difficult to predict and manage (Scheffer et al., 2009).
50 Such 'critical' transitions have been detected mostly at local scales (S. R. Carpenter et al., 2011; Drake &
51 Griffen, 2010), but the accumulation of changes in local communities that overlap geographically can prop-
52 agate and theoretically cause an abrupt change of the entire system at larger scales (Barnosky et al., 2012).
53 Coupled with the existence of global scale forcings, this implies the possibility that a critical transition could
54 occur at a global scale (C. Folke et al., 2011; Rockstrom et al., 2009).

55 Complex systems can experience two general classes of critical transitions (R V Solé, 2011). In so-called first
56 order transitions, a catastrophic regime shift that is mostly irreversible occurs because of the existence of
57 alternative stable states (Scheffer et al., 2001). This class of transitions is suspected to be present in a variety
58 of ecosystems such as lakes, woodlands, coral reefs (Scheffer et al., 2001), semi-arid grasslands (Brandon T.
59 Bestelmeyer et al., 2011), and fish populations (Vasilakopoulos & Marshall, 2015). They can be the result of
60 positive feedback mechanisms (Villa Martín, Bonachela, Levin, & Muñoz, 2015); for example, fires in some
61 forest ecosystems were more likely to occur in previously burned areas than in unburned places (Kitzberger,
62 Aráoz, Gowda, Mermoz, & Morales, 2012).

63 The other class of critical transitions are continuous or second order transitions (Ricard V. Solé & Bascompte,
64 2006). In these cases, there is a narrow region where the system suddenly changes from one domain to another,
65 with the change being continuous and in theory reversible. This kind of transitions were suggested to be
66 present in tropical forest (S. Pueyo et al., 2010), semi-arid mountain ecosystems (McKenzie & Kennedy,
67 2012), tundra shrublands (Naito & Cairns, 2015). The transition happens at a critical point where we can
68 observe a distinctive spatial pattern: scale invariant fractal structures characterized by power law patch
69 distributions (Stauffer & Aharony, 1994).

70 There are several processes that can convert a catastrophic transition to a second order transitions (Villa
71 Martín et al., 2015). These include stochasticity, such as demographic fluctuations, spatial heterogeneities,
72 and/or dispersal limitation. All these components are present in forest around the globe (Filotas et al.,
73 2014; Fung, O'Dwyer, Rahman, Fletcher, & Chisholm, 2016; Seidler & Plotkin, 2006), and thus continuous
74 transitions might be more probable than catastrophic transitions. Moreover there is some evidence of recovery
75 in some systems that supposedly suffered an irreversible transition produced by overgrazing (Brandon T
76 Bestelmeyer, Duniway, James, Burkett, & Havstad, 2013; J. Y. Zhang, Wang, Zhao, Xie, & Zhang, 2005)
77 and desertification (Allington & Valone, 2010).

78 The spatial phenomena observed in continuous critical transitions deal with connectivity, a fundamental
79 property of general systems and ecosystems from forests (Ochoa-Quintero, Gardner, Rosa, de Barros Ferraz,
80 & Sutherland, 2015) to marine ecosystems (Leibold & Norberg, 2004) and the whole biosphere (Lenton &
81 Williams, 2013). When a system goes from a fragmented to a connected state we say that it percolates (R
82 V Solé, 2011). Percolation implies that there is a path of connections that involves the whole system. Thus
83 we can characterize two domains or phases: one dominated by short-range interactions where information
84 cannot spread, and another in which long range interactions are possible and information can spread over
85 the whole area. (The term “information” is used in a broad sense and can represent species dispersal or
86 movement.)

87 Thus, there is a critical “percolation threshold” between the two phases, and the system could be driven close
88 to or beyond this point by an external force; climate change and deforestation are the main forces that could
89 be the drivers of such a phase change in contemporary forests (Bonan, 2008; Haddad et al., 2015). There
90 are several applications of this concept in ecology: species' dispersal strategies are influenced by percolation
91 thresholds in three-dimensional forest structure (Ricard V Solé, Bartumeus, & Gamarra, 2005), and it has
92 been shown that species distributions also have percolation thresholds (He & Hubbell, 2003). This implies
93 that pushing the system below the percolation threshold could produce a biodiversity collapse (J. Bascompte
94 & Solé, 1996; Pardini, Bueno, Gardner, Prado, & Metzger, 2010; Ricard V. Solé, Alonso, & Saldaña, 2004);

95 conversely, being in a connected state (above the threshold) could accelerate the invasion of forest into prairie
96 (Loehle, Li, & Sundell, 1996; Naito & Cairns, 2015).

97 One of the main challenges with systems that can experience critical transitions—of any kind—is that the
98 value of the critical threshold is not known in advance. In addition, because near the critical point a small
99 change can precipitate a state shift of the system, they are difficult to predict. Several methods have been
100 developed to detect if a system is close to the critical point, e.g. a deceleration in recovery from perturbations,
101 or an increase in variance in the spatial or temporal pattern (Boettiger & Hastings, 2012; S. R. Carpenter
102 et al., 2011; Dai, Vorselen, Korolev, & Gore, 2012; Hastings & Wysham, 2010).

103 The existence of a critical transition between two states has been established for forest at global scale in
104 different works (Hirota, Holmgren, Nes, & Scheffer (2011); Verbesselt et al. (2016); Staal, Dekker, Xu, &
105 Nes (2016); Wuyts, Champneys, & House (2017)). It was not probed, but is generally believed, that this
106 constitutes a first order catastrophic transition. The regions where forest can grow are not distributed
107 homogeneously, there are demographic fluctuations in forest growth and disturbances produced by human
108 activities. Due to new theoretical advances (Villa Martín, Bonachela, & Muñoz, 2014; Villa Martín et al.,
109 2015) all these factors imply that if these were first order transitions they will be converted or observed as
110 second order continuous transitions. From this basis we applied indices derived from second order transitions
111 to global forest cover dynamics.

112 In this study, our objective is to look for evidence that forests around the globe are near continuous critical
113 point that represent a fragmentation threshold. We use the framework of percolation to first evaluate if
114 forest patch distribution at a continental scale is described by a power law distribution and then examine
115 the fluctuations of the largest patch. The advantage of using data at a continental scale is that for very
116 large systems the transitions are very sharp (R V Solé, 2011) and thus much easier to detect than at smaller
117 scales, where noise can mask the signals of the transition.

118 Methods

119 Study areas definition

120 We analyzed mainland forests at a continental scale, covering the whole globe, by delimiting land areas with
121 a near-contiguous forest cover, separated with each other by large non-forested areas. Using this criterion,
122 we delimited the following forest regions. In America, three regions were defined: South America temperate
123 forest (SAT), subtropical and tropical forest up to Mexico (SAST), and USA and Canada forest (NA). Europe

124 and North Asia were treated as one region (EUAS). The rest of the delimited regions were South-east Asia
125 (SEAS), Africa (AF), and Australia (OC). We also included in the analysis islands larger than 10^5 km^2 . The
126 mainland region has the number 1 e.g. OC1, and the nearby islands have consecutive numeration (Appendix
127 S4, figure S1-S6).

128 Forest patch distribution

129 We studied forest patch distribution in each defined area from 2000 to 2015 using the MODerate-resolution
130 Imaging Spectroradiometer (MODIS) Vegetation Continuous Fields (VCF) Tree Cover dataset version 051
131 (C. DiMiceli et al., 2015). This dataset is produced at a global level with a 231-m resolution, from 2000
132 onwards on an annual basis. There are several definition of forest based on percent tree cover (J. O. Sexton
133 et al., 2015); we choose a range from 20% to 30% threshold in 5% increments to convert the percentage
134 tree cover to a binary image of forest and non-forest pixels. This range is centered in the definition used by
135 the United Nations' International Geosphere-Biosphere Programme (Belward, 1996), and studies of global
136 fragmentation (Haddad et al., 2015) and includes the range used in other studies of critical transitions (Xu
137 et al., 2016). Using this range we try to avoid the errors produced by low discrimination of MODIS VCF
138 between forest and dense herbaceous vegetation at low forest cover and the saturation of MODIS VCF in
139 dense forests (J. O. Sexton et al., 2013). We repeat all the analysis described below for this set of thresholds,
140 except in some specific cases described below. Patches of contiguous forest were determined in the binary
141 image by grouping connected forest pixels using a neighborhood of 8 forest units (Moore neighborhood).
142 The MODIS VCF product defines the percentage of tree cover by pixel, but does not discriminate the type
143 of trees so besides natural forest it includes plantations of tree crops like rubber, oil palm, ecualyptus and
144 others.

145 Percolation theory

146 A more in-depth introduction to percolation theory can be found elsewhere (Stauffer & Aharony, 1994) and
147 a review from an ecological point of view is available (B. Oborny, Szabó, & Meszéna, 2007). Here, to explain
148 the basic elements of percolation theory we formulate a simple model: we represent our area of interest by a
149 square lattice and each site of the lattice can be occupied—e.g. by forest—with a probability p . The lattice
150 will be more occupied when p is greater, but the sites are randomly distributed. We are interested in the
151 connection between sites, so we define a neighborhood as the eight adjacent sites surrounding any particular
152 site. The sites that are neighbors of other occupied sites define a patch. When there is a patch that connects

153 the lattice from opposite sides, it is said that the system percolates. When p is increased from low values, a
154 percolating patch suddenly appears at some value of p called the critical point p_c .

155 Thus percolation is characterized by two well defined phases: the unconnected phase when $p < p_c$ (called
156 subcritical in physics), in which species cannot travel far inside the forest, as it is fragmented; in a general
157 sense, information cannot spread. The second is the connected phase when $p > p_c$ (supercritical), species
158 can move inside a forest patch from side to side of the area (lattice), i.e. information can spread over the
159 whole area. Near the critical point several scaling laws arise: the structure of the patch that spans the area
160 is fractal, the size distribution of the patches is power-law, and other quantities also follow power-law scaling
161 (Stauffer & Aharony, 1994).

162 The value of the critical point p_c depends on the geometry of the lattice and on the definition of the
163 neighborhood, but other power-law exponents only depend on the lattice dimension. Close to the critical
164 point, the distribution of patch sizes is:

165 (1) $n_s(p_c) \propto s^{-\alpha}$

166 where $n_s(p)$ is the number of patches of size s . The exponent α does not depend on the details of the
167 model and it is called universal (Stauffer & Aharony, 1994). These scaling laws can be applied for landscape
168 structures that are approximately random, or at least only correlated over short distances (Gastner, Oborny,
169 Zimmermann, & Pruessner, 2009). In physics this is called “isotropic percolation universality class”, and
170 corresponds to an exponent $\alpha = 2.05495$. If we observe that the patch size distribution has another exponent
171 it will not belong to this universality class and some other mechanism should be invoked to explain it.
172 Percolation thresholds can also be generated by models that have some kind of memory (Hinrichsen, 2000;
173 Ódor, 2004): for example, a patch that has been exploited for many years will recover differently than a
174 recently deforested forest patch. In this case, the system could belong to a different universality class, or in
175 some cases there is no universality, in which case the value of α will depend on the parameters and details
176 of the model (Corrado, Cherubini, & Pennetta, 2014).

177 To illustrate these concepts, we conducted simulations with a simple forest model with only two states: forest
178 and non-forest. This type of model is called a “contact process” and was introduced for epidemics (Harris,
179 1974), but has many applications in ecology (Gastner et al., 2009; Ricard V. Solé & Bascompte, 2006). A
180 site with forest can become extinct with probability e , and produce another forest site in a neighborhood
181 with probability c . We use a neighborhood defined by an isotropic power law probability distribution. We
182 defined a single control parameter as $\lambda = c/e$ and ran simulations for the subcritical fragmentation state
183 $\lambda < \lambda_c$, with $\lambda = 2$, near the critical point for $\lambda = 2.5$, and for the supercritical state with $\lambda = 5$ (see

184 supplementary data, gif animations).

185 **Patch size distributions**

186 We fitted the empirical distribution of forest patches calculated for each of the thresholds on the range
187 we previously mentioned. We used maximum likelihood (Clauset, Shalizi, & Newman, 2009; Goldstein,
188 Morris, & Yen, 2004) to fit four distributions: power-law, power-law with exponential cut-off, log-normal,
189 and exponential. We assumed that the patch size distribution is a continuous variable that was discretized
190 by remote sensing data acquisition procedure.

191 We set a minimal patch size (X_{min}) at nine pixels to fit the patch size distributions to avoid artifacts at patch
192 edges due to discretization (Weerman et al., 2012). Besides this hard X_{min} limit we set due to discretization,
193 the power-law distribution needs a lower bound for its scaling behavior. This lower bound is also estimated
194 from the data by maximizing the Kolmogorov-Smirnov (KS) statistic, computed by comparing the empirical
195 and fitted cumulative distribution functions (Clauset et al., 2009). For the log-normal model we constrain
196 the values of the μ parameter to positive values, this parameter controls the mode of the distribution and
197 when is negative most of the probability density of the distribution lies outside the range of the forest patch
198 size data (Limpert, Stahel, & Abbt, 2001).

199 To select the best model we calculated corrected Akaike Information Criteria (AIC_c) and Akaike weights for
200 each model (Burnham & Anderson, 2002). Akaike weights (w_i) are the weight of evidence in favor of model
201 i being the actual best model given that one of the N models must be the best model for that set of N
202 models. Additionally, we computed a likelihood ratio test (Clauset et al., 2009; Vuong, 1989) of the power
203 law model against the other distributions. We calculated bootstrapped 95% confidence intervals (Crawley,
204 2012) for the parameters of the best model; using the bias-corrected and accelerated (BCa) bootstrap (Efron
205 & Tibshirani, 1994) with 10000 replications.

206 **Largest patch dynamics**

207 The largest patch is the one that connects the highest number of sites in the area. This has been used
208 extensively to indicate fragmentation (R. H. Gardner & Urban, 2007; Ochoa-Quintero et al., 2015). The
209 relation of the size of the largest patch S_{max} to critical transitions has been extensively studied in relation
210 to percolation phenomena (Bazant, 2000; Botet & Ploszajczak, 2004; Stauffer & Aharony, 1994), but seldom
211 used in ecological studies (for an exception see Gastner et al. (2009)). When the system is in a connected
212 state ($p > p_c$) the landscape is almost insensitive to the loss of a small fraction of forest, but close to the

critical point a minor loss can have important effects (B. Oborny et al., 2007; Ricard V. Solé & Bascompte, 2006), because at this point the largest patch will have a filamentary structure, i.e. extended forest areas will be connected by thin threads. Small losses can thus produce large fluctuations.

One way to evaluate the fragmentation of the forest is to calculate the proportion of the largest patch against the total area (Keitt, Urban, & Milne, 1997). The total area of the regions we are considering (Appendix S4, figures S1-S6) may not be the same than the total area that the forest could potentially occupy, thus a more accurate way to evaluate the weight of S_{max} is to use the total forest area, that can be easily calculated summing all the forest pixels. We calculate the proportion of the largest patch for each year, dividing S_{max} by the total forest area of the same year: $RS_{max} = S_{max}/\sum_i S_i$. This has the effect of reducing the S_{max} fluctuations produced due to environmental or climatic changes influences in total forest area. When the proportion RS_{max} is large (more than 60%) the largest patch contains most of the forest so there are fewer small forest patches and the system is probably in a connected phase. Conversely, when it is low (less than 20%), the system is probably in a fragmented phase (Saravia & Momo, 2017). As we calculated these largest patch indices for different thresholds, the values of the total forest area and the value of S_{max} are lower as threshold is higher, we expect that the value of RS_{max} will change and probably be lower at high thresholds. To define if a region will be in a connected or unconnected state we used the RS_{max} of the highest threshold (40%) which is more conservative to evaluate the risk of fragmentation and includes the most dense forest area. Additionally if RS_{max} is a good indicator of the fragmented or unfragmented state of the forest and these are the two alternative states for the critical transition the RS_{max} distribution of frequencies should be bimodal (Brandon T. Bestelmeyer et al., 2011); so we apply the Hartigan's dip test that measures departures from unimodality (J. A. Hartigan & Hartigan, 1985).

The RS_{max} is a useful qualitative index that does not tell us if the system is near or far from the critical transition; this can be evaluated using the temporal fluctuations. We calculate the fluctuations around the mean with the absolute values $\Delta S_{max} = S_{max}(t) - \langle S_{max} \rangle$, using the proportions of RS_{max} . To characterize fluctuations we fitted three empirical distributions: power-law, log-normal, and exponential, using the same methods described previously. We expect that large fluctuation near a critical point have heavy tails (log-normal or power-law) and that fluctuations far from a critical point have exponential tails, corresponding to Gaussian processes (Rooij, Nash, Rajaraman, & Holden, 2013). As the data set spans 16 years, it is probable that will do not have enough power to reliably detect which distribution is better (Clauset et al., 2009). To improve this we used the same likelihood ratio test we used previously (Clauset et al., 2009; Vuong, 1989); if the p-value obtained to compare the best distribution against the others we concluded that there is not enough data to decide which is the best model. We generated animated maps showing the fluctuations of

245 the two largest patches at 30% threshold, to aid in the interpretations of the results.

246 A robust way to detect if the system is near a critical transition is to analyze the increase in variance of
247 the density (Benedetti-Cecchi, Tamburello, Maggi, & Bulleri, 2015). It has been demonstrated that the
248 variance increase in density appears when the system is very close to the transition (Corrado et al., 2014),
249 thus practically it does not constitute an early warning indicator. An alternative is to analyze the variance of
250 the fluctuations of the largest patch ΔS_{max} : the maximum is attained at the critical point but a significant
251 increase occurs well before the system reaches the critical point (Corrado et al., 2014; Saravia & Momo,
252 2017). In addition, before the critical fragmentation, the skewness of the distribution of ΔS_{max} should be
253 negative, implying that fluctuations below the average are more frequent. We characterized the increase in
254 the variance using quantile regression: if variance is increasing the slopes of upper or/and lower quartiles
255 should be positive or negative.

256 All statistical analyses were performed using the GNU R version 3.3.0 (R Core Team, 2015), to fit the
257 distributions of patch sizes we used the Python package powerlaw (Alstott, Bullmore, & Plenz, 2014). For
258 the quantile regressions we used the R package quantreg (Koenker, 2016). Image processing was done
259 in MATLAB r2015b (The Mathworks Inc.). The complete source code for image processing and statistical
260 analysis, and the patch size data files are available at figshare <http://dx.doi.org/10.6084/m9.figshare.4263905>.

261 Results

262 The figure 1 shows an example of the distribution of the biggest 200 patches for years 2000 and 2014, this
263 distribution is highly variable, but the biggest patch usually maintains its place. Sometimes the biggest
264 patch breaks and then big fluctuations in its size are observed, as we will analyze below. Smaller patches
265 can merge or break more easily so they enter or leave the list of 200, and this is why there is a color change
266 across years.

267 The power law distribution was selected as the best model in 99% of the cases (Figure S7). In a small
268 number of cases (1%) the power law with exponential cutoff was selected, but the value of the parameter α
269 was similar by ± 0.03 to the pure power law (Table S1, and model fit data table). Additionally the patch size
270 where the exponential tail begins is very large, thus we used the power law parameters for this cases (region
271 EUAS3,SAST2). In finite-size systems the favored model should be the power law with exponential cut-off,
272 because the power-law tails are truncated to the size of the system (Stauffer & Aharony, 1994). This implies
273 that differences between the two kinds of power law models should be small. We observed that phenomena:
274 when the pure power-law model is selected as the best model the likelihood ratio test shows that in 64% of

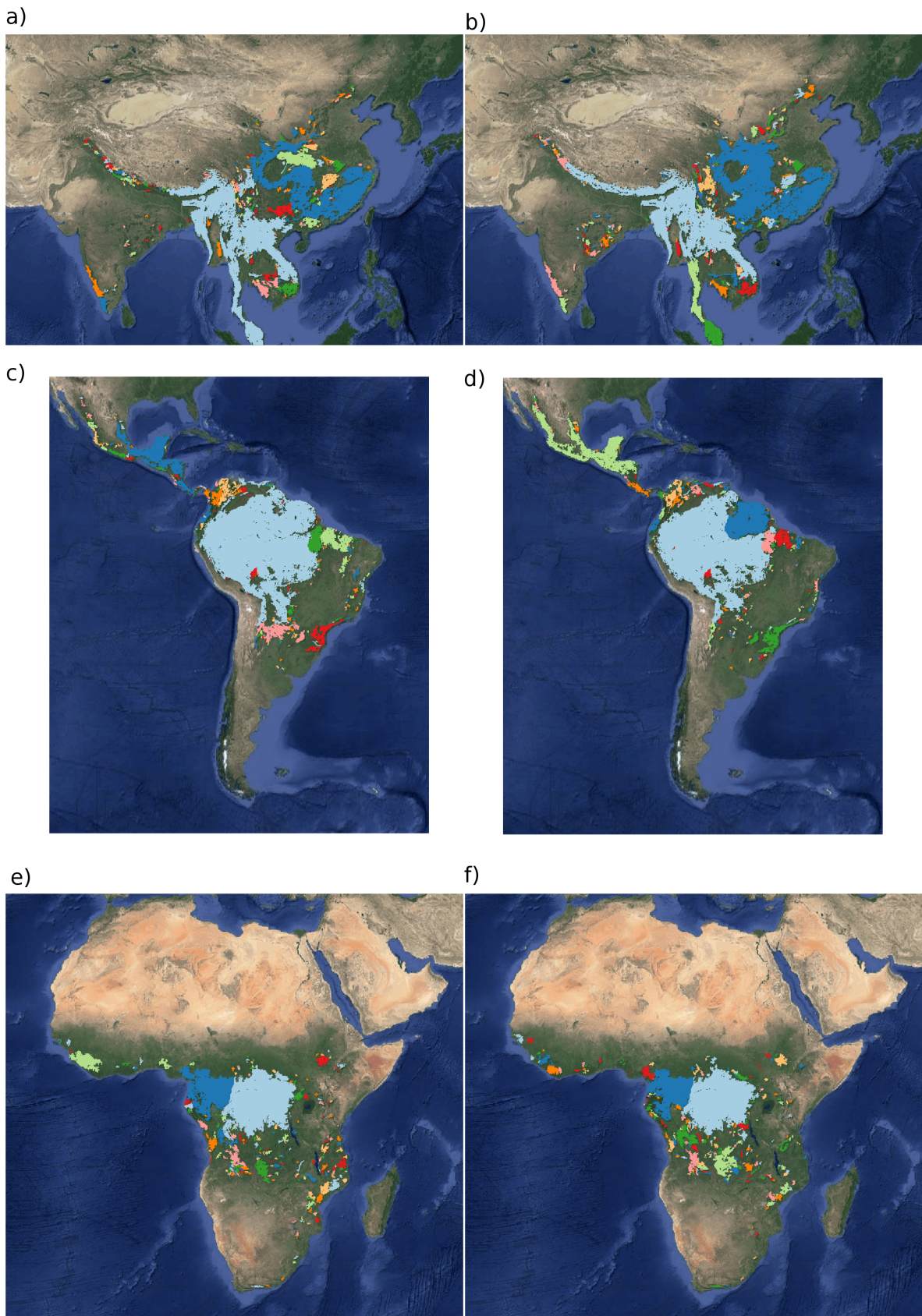


Figure 1: Forest patch distributions for continental regions for the years 2000 and 2014. The images are the 200 biggest patches, showed at a coarse pixel scale of 2.5 km. The regions are: a) & b) southeast Asia; c) & d) South America subtropical and tropical and e) & f) Africa mainland, for the years 2000 and 2014 respectively. The color palette was chosen to discriminate different patches and do not represent patch size.

275 the cases the differences with power law with exponential cutoff are not significant (p-value>0.05); in these
276 cases the differences between the fitted α for both models are less than 0.001. Instead the likelihood ratio
277 test clearly differentiates the power law model from the exponential model (100% cases p-value<0.05), and
278 the log-normal model (90% cases p-value<0.05).

279 The global mean of the power-law exponent α is 1.967 and the bootstrapped 95% confidence interval is 1.964
280 - 1.970. Besides that, the global values for each threshold are different, because their confidence intervals
281 do not overlap, and their range goes from 1.90 to 2.01 (Table S1). Analyzing the biggest regions (Figure
282 1, Table S2) the north hemisphere (EUAS1 & NA1) have similar values of α (1.97, 1.98), pantropical areas
283 have different α with greatest values for South America (SAST1, 2.01) and in descending order Africa (AF1,
284 1.946) and Southeast Asia (SEAS1, 1.895). With greater α the fluctuations of patch sizes are lower and vice
285 versa (M. E. J. Newman, 2005).

286 We calculated the total areas of forest and the largest patch S_{max} by year for different thresholds; as expected
287 these two values increase for smaller thresholds (Table S3). We expect less variations in the largest patch
288 relative to total forest area RS_{max} (Figure S9); in ten cases it keeps near or higher than 60% (EUAS2, NA5,
289 OC2, OC3, OC4, OC5, OC6, OC8, SAST1, SAT1) over the 25-35 range or more. In four cases it keeps
290 around 40% or less at least over the 25-30% range (AF1, EUAS3, OC1, SAST2) and in six cases there is
291 a crossover from more than 60% to around 40% or less (AF2, EUAS1, NA1, OC7, SEAS1, SEAS2). This
292 confirms the criteria of using the most conservative threshold value of 40% to interpret RS_{max} with regard
293 to the fragmentation state of the forest. The frequency of RS_{max} showed bimodality (Figure 3) and the dip
294 test rejected unimodality ($D = 0.0416$, p-value = 0.0003), which also indicates RS_{max} as a good index to
295 study the fragmentation state of the forest.

296 The RS_{max} for regions with more than 10^7 km² of forest is shown in figure 4. South America tropical and
297 subtropical (SAST1) is the only region with an average close to 60%, the other regions are below 30%. Eurasia
298 mainland (EUAS1) has the lowest value near 20%. For regions with less total forest area (Figure S10, Table
299 S3), Great Britain (EUAS3) has the lowest proportion less than 5%, Java (OC7) and Cuba (SAST2) are
300 under 25%, while other regions such as New Guinea (OC2), Malaysia/Kalimantan (OC3), Sumatra (OC4),
301 Sulawesi (OC5) and South New Zealand (OC6) have a very high proportion (75% or more). Philippines
302 (SEAS2) seems to be a very interesting case because it seems to be under 30% until the year 2007, fluctuates
303 around 30% in years 2008-2010, then jumps near 60% in 2011-2013 and then falls again to 30%, this seems
304 an example of a transition from a fragmented state to a unfragmented one (figure S10).

305 We analyzed the distributions of fluctuations of the largest patch relative to total forest area ΔRS_{max} and

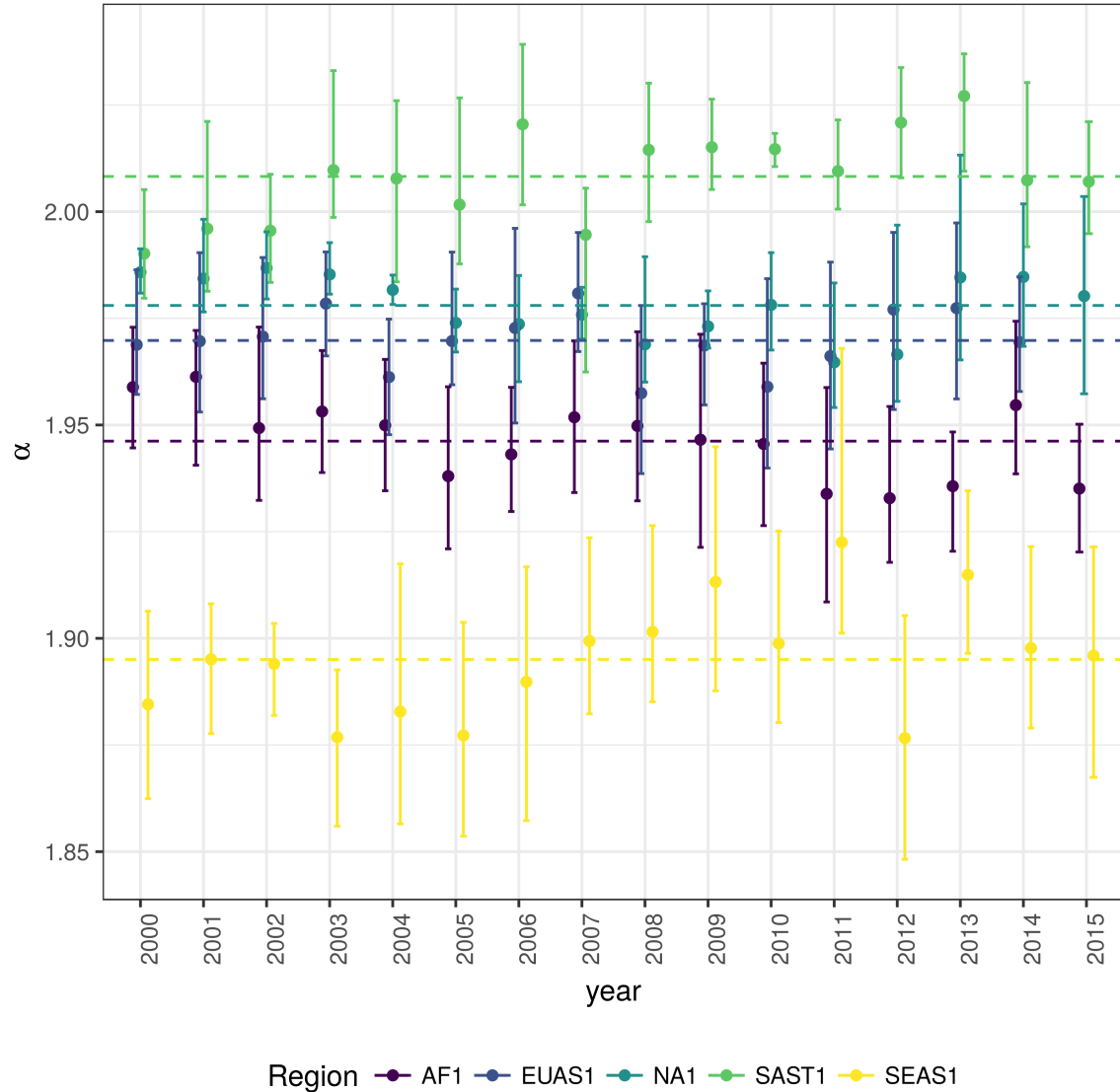


Figure 2: Power law exponents (α) of forest patch distributions for regions with total forest area $> 10^7 \text{ km}^2$. Dashed horizontal lines are the means by region, with 95% confidence interval error bars estimated by bootstrap resampling. The regions are AF1: Africa mainland, EUAS1: Eurasia mainland, NA1: North America mainland, SAST1: South America subtropical and tropical, SEAS1: Southeast Asia mainland.

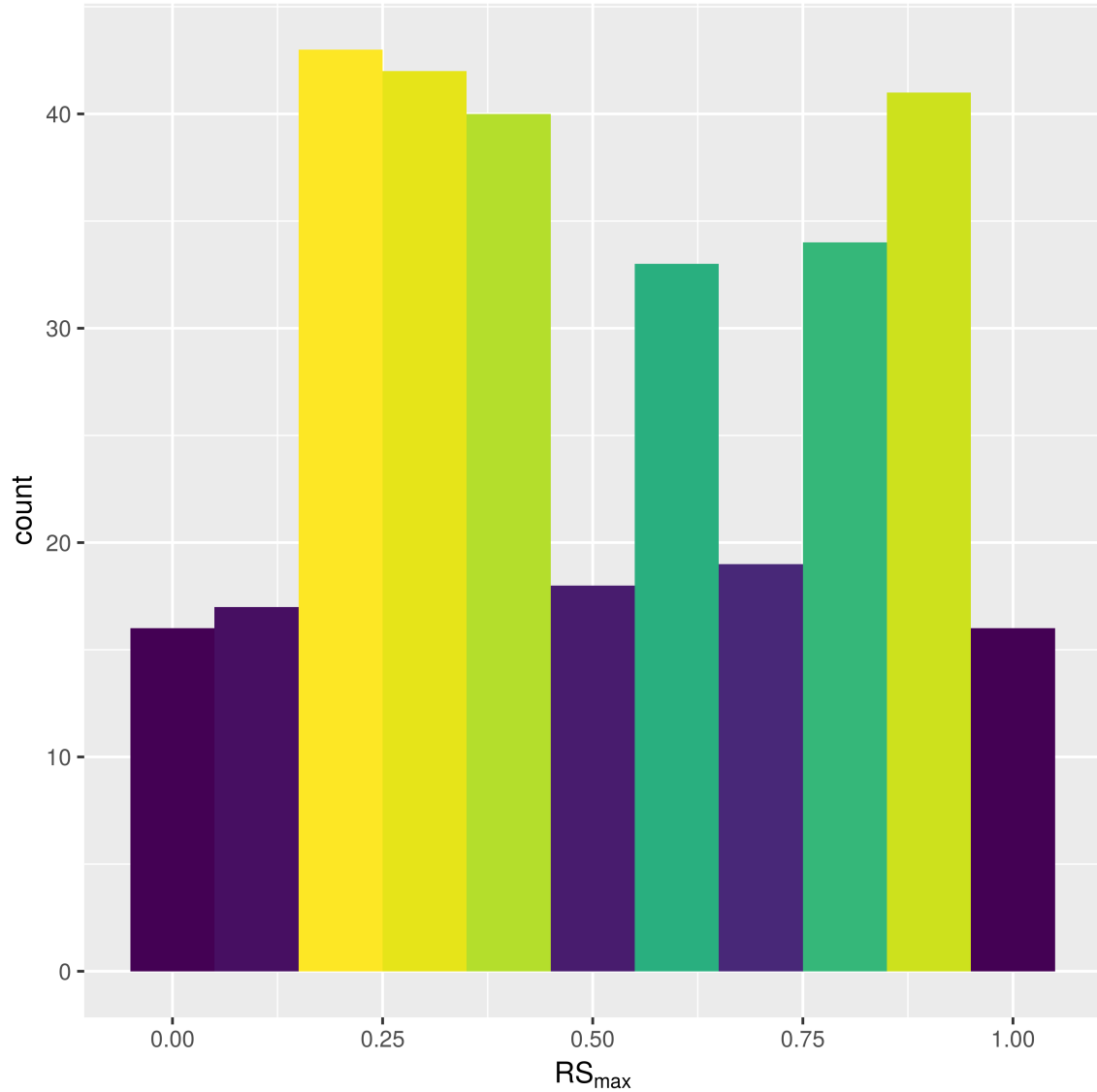


Figure 3: Frequency distribution of Largest patch proportion relative to total forest area RS_{max} calculated using a threshold of 40% of forest in each pixel to determine patches. Bimodality is observed and confirmed by the dip test ($D = 0.0416$, $p\text{-value} = 0.0003$). This indicates the existence of two states needed for a critical transition.

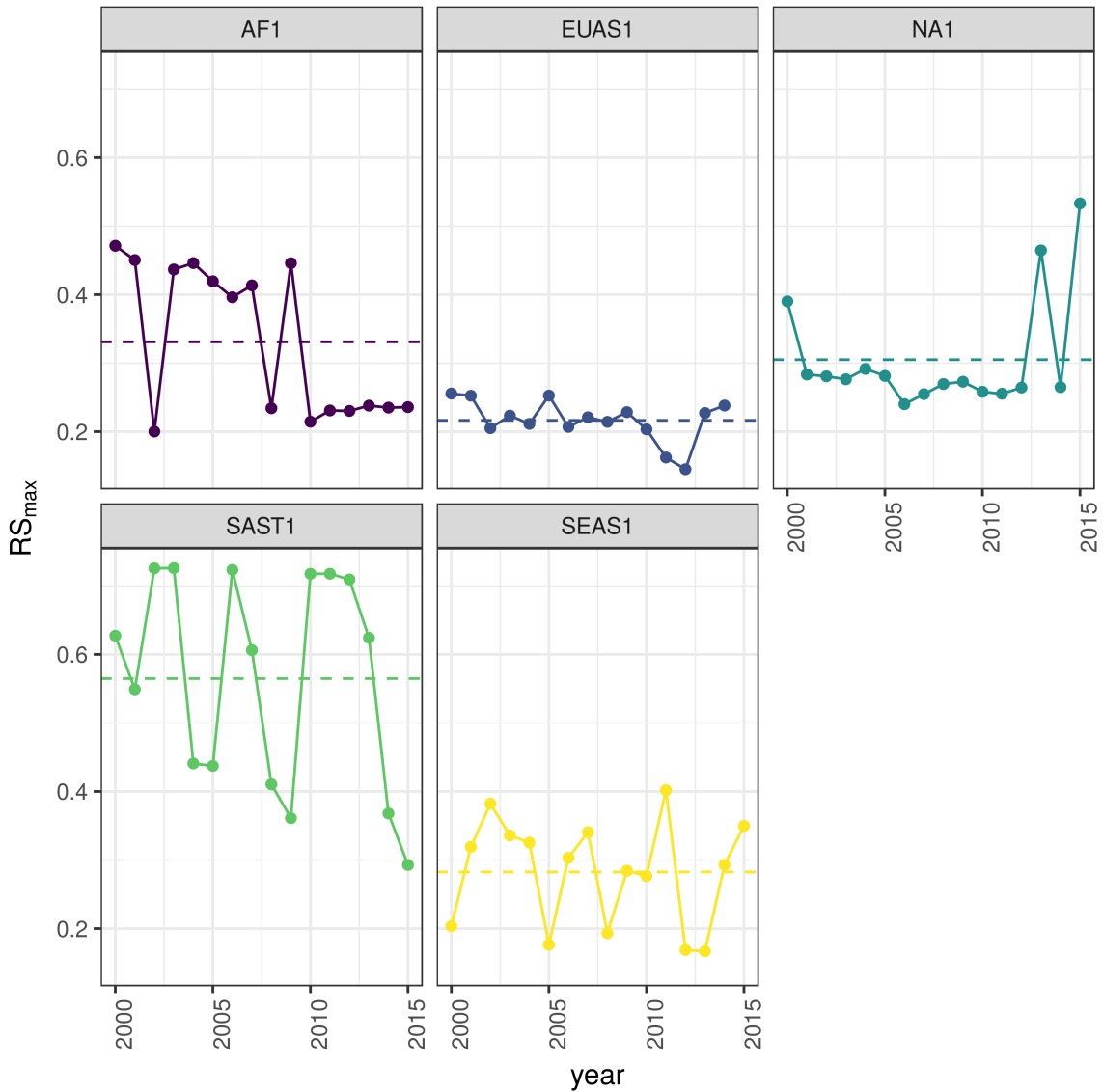


Figure 4: Largest patch proportion relative to total forest area RS_{max} , for regions with total forest area $> 10^7 \text{ km}^2$. We show here the RS_{max} calculated using a threshold of 40% of forest in each pixel to determine patches. Dashed lines are averages across time. The regions are AF1: Africa mainland, EUAS1: Eurasia mainland, NA1: North America mainland, SAST1: South America tropical and subtropical, SEAS1: Southeast Asia mainland.

306 the fluctuations of the largest patch ΔS_{max} . Besides the Akaike criteria identified different distributions as
307 the best, in most cases the Likelihood ratio test is not significant thus the data is not enough to determine
308 with confidence which is the best distribution. Only 1 case the distribution selected by the Akaike criteria is
309 confirmed as the correct model for relative and absolute fluctuations (Table S4). Thus we do not apply this
310 criteria because is not informative, we can not decide with reliability if the best distribution is the selected
311 one.

312 The animations of the two largest patches (see supplementary data, largest patch gif animations) qualitatively
313 shows the nature of fluctuations and if the state of the forest is connected or not. If the largest patch is
314 always the same patch over time, the forest is probably not fragmented; this happens for regions with RS_{max}
315 of more than 40% such as AF2 (Madagascar), EUAS2 (Japan), NA5 (Newfoundland) and OC3 (Malaysia).
316 In the regions with RS_{max} between 40% and 30% the identity of the largest patch could change or stay the
317 same in time. For OC7 (Java) the largest patch changes and for AF1 (Africa mainland) it stays the same.
318 Only for EUAS1 (Eurasia mainland) we observed that the two largest patches are always the same, implying
319 that this region is probably composed of two independent domains and should be divided in further studies.
320 The regions with RS_{max} less than 25%: SAST2 (Cuba) and EUAS3 (Great Britain), the largest patch always
321 changes reflecting their fragmented state. In the case of SEAS2 (Philippines) a transition is observed, with
322 the identity of the largest patch first variable, and then constant after 2010.

323 The results of quantile regressions are almost identical for ΔRS_{max} and ΔS_{max} (table S5); in very few cases
324 only one of them is significant but we only take into account results where both are significant. Among the
325 biggest regions, Africa (AF1) has a similar pattern across thresholds but only at 30% threshold is significant;
326 the upper and lower quantiles have significant negative slopes, but the lower quantile slope is lower, implying
327 that negative fluctuations and variance are increasing (Figure 5). Eurasia mainland (EUAS1) has significant
328 slopes at 20%, 30% and 40% thresholds but the patterns are different at 20% variance is decreasing, at 30%
329 and 40% only is increasing. This is because the largest patch is composed of pixels with different cover
330 of forest, thus there are more variation in pixels from 30% to 20% than from 20% to less than 20%, then
331 the fluctuations are happening between 40% and 20%. The signal is that the variation of the most dense
332 portion of the largest patch is increasing withing a limited range. North America mainland (NA1) exhibits
333 the same pattern at 20%, 25% and 30% thresholds: a significant lower quantile with positive slope, implying
334 decreasing variance. South America tropical and subtropical (SAST1) have significant lower quantile with
335 negative slope at 25% and 30% thresholds indicating an increase in variance. Finally, SEAS1 have a upper
336 quantile with positive slope significant for 25% threshold, also indicating an increasing variance. The other
337 regions, with forest area smaller than 10^7 km^2 are showed in figure S11 and table S5. Philippines (SEAS2)

338 is an interesting case: the slopes of lower quantils are positive for thresholds 20% and 25%, and the upper
339 quantil slopes are positive for thresholds 30% and 40%; thus variance is decreasing at 20%-25% and increasing
340 at 30%-40%.

341 The conditions that indicate that a region is near a critical fragmentation threshold are that patch size
342 distributions follow a power law; variance of ΔRS_{max} is increasing in time; and skewness is negative. All
343 these conditions must happen at the same time at least for one threshold. When the threshold is higher more
344 dense regions of the forest are at risk. This happens for Africa mainland (AF1), Eurasia mainland(EUAS1),
345 Japan (EUAS2), Australia mainland (OC1), Malaysia/Kalimantan (OC3), Sumatra (OC4), South America
346 tropical & subtropical (SAST1), Cuba (SAST2), Southeast Asia, Mainland (SEAS1).

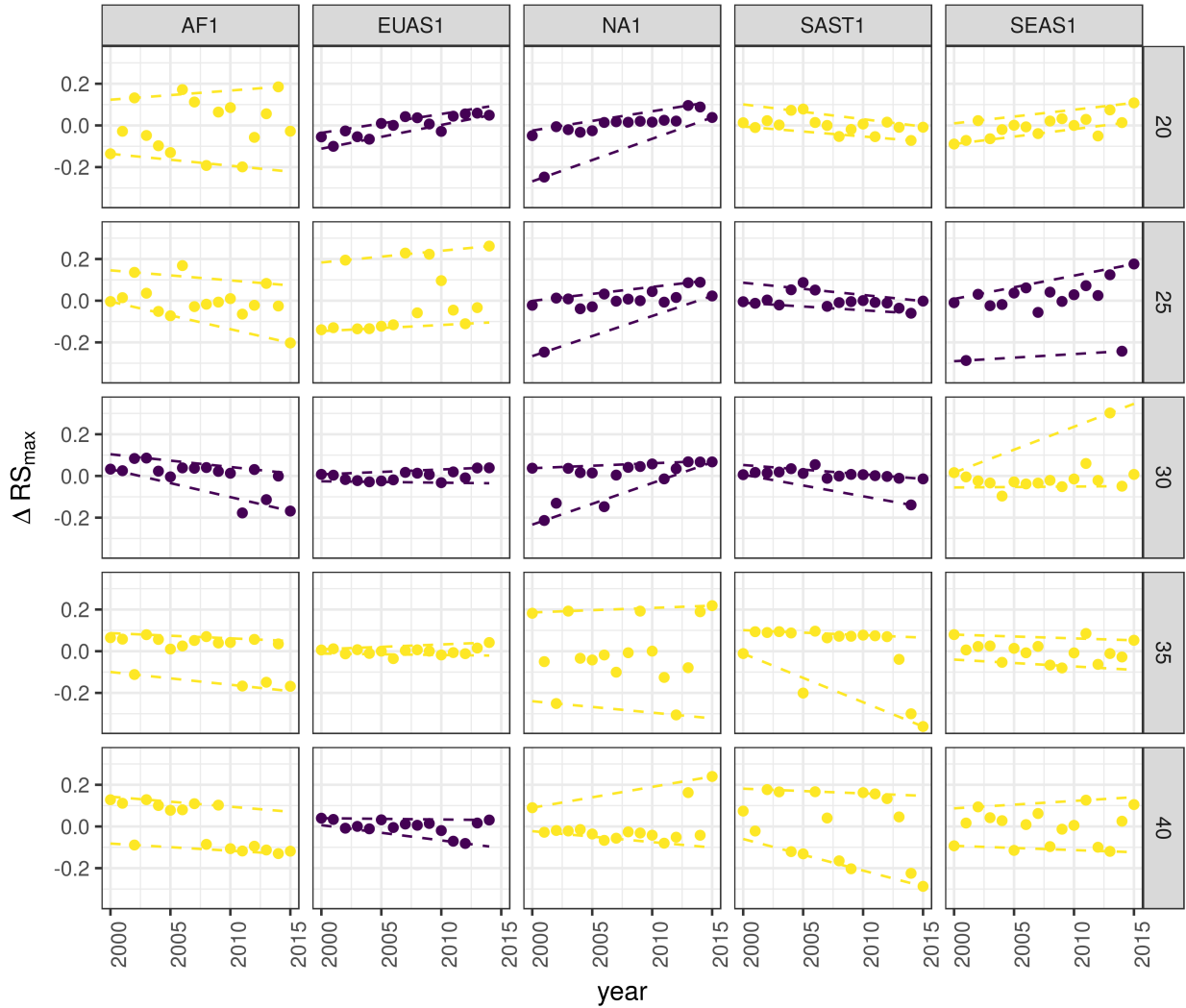


Figure 5: Largest patch fluctuations for regions with total forest area $> 10^7 \text{ km}^2$ across years. The patch sizes are relative to the total forest area of the same year. Dashed lines are 90% and 10% quantile regressions, to show if fluctuations were increasing; purple (dark) panels have significant slopes. The regions are AF1: Africa mainland, EUAS1: Eurasia mainland, NA1: North America mainland, SAST1: South America tropical and subtropical, SEAS1: Southeast Asia mainland.

Table 1: Regions and indicators of closeness to a critical fragmentation point. Where: RS_{max} is the largest patch divided by the total forest area; Threshold is the value used to calculate patches from the MODIS VCF pixels; ΔRS_{max} are the fluctuations of RS_{max} around the mean and the increase or decrease in the variance was estimated using quantile regressions; skewness was calculated for RS_{max} . NS means the results were non-significant. The conditions that determine the closeness to a fragmentation point are: increasing variance of ΔRS_{max} and negative skewness. RS_{max} indicates if the forest is unfragmented (>0.6) or fragmented (<0.3).

Region	Description	RS_{max}	Threshold	Variance of ΔRS_{max}	Skewness
AF1	Africa mainland	0.33	30	Increase	-1.4653
AF2	Madagascar	0.48	20	Increase	0.7226
EUAS1	Eurasia, mainland	0.22	20	Decrease	-0.4814
EUAS1			30	Increase	0.3113
EUAS1			40	Increase	-1.2790
EUAS2	Japan	0.94	35	Increase	-0.3913
EUAS2			40	Increase	-0.5030
EUAS3	Great Britain	0.03	40	NS	
NA1	North America, mainland	0.31	20	Decrease	-2.2895
NA1			25	Decrease	-2.4465
NA1			30	Decrease	-1.6340
NA5	Newfoundland	0.54	40	NS	
OC1	Australia, Mainland	0.36	30	Increase	0.0920
OC1			35	Increase	-0.8033
OC2	New Guinea	0.96	25	Decrease	-0.1003
OC2			30	Decrease	0.1214
OC2			35	Decrease	-0.0124
OC3	Malaysia/Kalimantan	0.92	35	Increase	-1.0147
OC3			40	Increase	-1.5649
OC4	Sumatra	0.84	20	Increase	-1.3846
OC4			25	Increase	-0.5887
OC4			30	Increase	-1.4226
OC5	Sulawesi	0.82	40	NS	
OC6	New Zealand South Island	0.75	40	Increase	0.3553
OC7	Java	0.16	40	NS	
OC8	New Zealand North Island	0.64	40	NS	
SAST1	South America, Tropical and Subtropical forest up to Mexico	0.56	25	Increase	1.0519
SAST1			30	Increase	-2.7216
SAST2	Cuba	0.15	20	Increase	0.5049
SAST2			25	Increase	1.7263
SAST2			30	Increase	0.1665
SAST2			40	Increase	-0.5401
SAT1	South America, Temperate forest	0.54	25	Decrease	0.1483
SAT1			30	Decrease	-1.6059
SAT1			35	Decrease	-1.3809
SEAS1	Southeast Asia, Mainland	0.28	25	Increase	-1.3328
SEAS2	Philippines	0.33	20	Decrease	-1.6373
SEAS2			25	Decrease	-0.6648
SEAS2			30	Increase	0.1517

Region	Description	RS_{max}	Threshold	Variance of ΔRS_{max}	Skewness
SEAS2			40	Increase	1.5996

347 Discussion

348 We found that the forest patch distribution of all regions of the world followed power laws spanning seven
 349 orders of magnitude. These include tropical rainforest, boreal and temperate forest. Power laws have
 350 previously been found for several kinds of vegetation, but never at global scales as in this study. Moreover
 351 the range of the estimated power law exponents is relatively narrow besides we used different thresholds
 352 (1.90 - 2.01). This suggest the existence of one unifying mechanism or different mechanism that act in the
 353 same way in different regions.

354 Several mechanisms have been proposed for the emergence of power laws in forest: the first is related self
 355 organized criticality (SOC), when the system is driven by its internal dynamics to a critical state; this has
 356 been suggested mainly for fire-driven forests (Hantson, Pueyo, & Chuvieco, 2015; Zinck & Grimm, 2009).
 357 Real ecosystems do not seem to meet the requirements of SOC dynamics because their are driven both
 358 endogenous and exogenous controls, non-homogeneous and they may not have the separation of time scales
 359 [Ricard V Solé, Alonso, & Mckane (2002);Sole2006]; furthermore there is some evidence that these conditions
 360 are not meet (McKenzie & Kennedy, 2012; S. Pueyo et al., 2010). A second possible mechanism, suggested
 361 by Pueyo et al. (2010), is isotropic percolation, when a system is near the critical point power law structures
 362 arise. This is equivalent to the random forest model that we explained previously, and requires the tuning
 363 of an external environmental condition to carry the system to this point. We did not expect forest growth
 364 to be a random process at local scales, but it is possible that combinations of factors cancel out to produce
 365 seemingly random forest dynamics at large scales. In this case we should have observed power laws in a
 366 limited set of situations that coincide with a critical point. The third mechanism suggested as the cause of
 367 pervasive power laws in patch size distribution is facilitation (Irvine, Bull, & Keeling, 2016; Manor & Shnerb,
 368 2008): a patch surrounded by forest will have a smaller probability of been deforested or degraded than an
 369 isolated patch. We hypothesize that models that include facilitation could explain the patterns observed here.
 370 The model of Scanlon et al. (2007) showed an $\alpha = 1.34$ which is different from our results (1.90 - 2.01 range).
 371 Another model but with three states (tree/non-tree/degraded), including local facilitation and grazing, was
 372 also used to obtain power laws patch distributions without external tuning, and exhibited deviations from
 373 power laws at high grazing pressures (S. Kéfi et al., 2007). The values of the power law exponent α obtained
 374 for this model are dependent on the intensity of facilitation, when facilitation is more intense the exponent

375 is higher, but the maximal values they obtained are still lower than the ones we observed. The interesting
376 point is that the value of the exponent is dependent on the parameters, and thus the observed α might be
377 obtained with some parameter combination.

378 The existence of a critical transitions in forest, mainly in neotropical forest to savanna, is a matter of
379 intense investigation, this is in general thought as first order or discontinuous transitions; we found power
380 laws in forest patch distributions which is a necessary but not a sufficient condition for a second order or
381 continuous transition. Is suggested that first order transitions do not even exists when the system is spatially
382 heterogeneous and present internal and external stochastic fluctuations as in forest; thus the application of
383 indices based on second order transitions seems to be justified.

384 It has been suggested that a combination of spatial and temporal indicators could more reliably detect
385 critical transitions (S. Kéfi et al., 2014). In this study, we combined five criteria to detect the closeness to
386 a fragmentation threshold. Two of them were spatial: the forest patch size distribution, and the proportion
387 of the largest patch relative to total forest area RS_{max} . The other three were the distribution of temporal
388 fluctuations in the largest patch size, the trend in the variance, and the skewness of the fluctuations. One
389 of them: the distribution of temporal fluctuations ΔRS_{max} can not be applied with our temporal resolution
390 due to the difficulties of fitting and comparing heavy tailed distributions. The combination of the remaining
391 four gives us an increased degree of confidence about the system being close to a critical transition. A power
392 law patch distribution can be indicative of a critical transition if it is present in a narrow range of conditions;
393 conversely if it is not found, the existence of a critical transition cannot be discarded. The monitoring of
394 biggest patches using RS_{max} is also important regardless the existence or not of critical transitions. RS_{max}
395 could be used to compare regions with different forest extension and as the total area of forest also change
396 with different environmental condition is at least partially independent of climatic conditions could be also
397 applied to compare forest from different latitudes. Moreover, RS_{max} contain most of the intact forest
398 landscapes defined by P. Potapov et al. (2008), thus it is a relatively simple way to evaluate the risk in these
399 areas.

400 We found that several continental only the tropical forest of Africa and South America met all five criteria,
401 and thus seem to be near a critical fragmentation threshold. This confirms previous studies that point to
402 these two tropical areas as the most affected by deforestation (M. C. Hansen et al., 2013). Africa seems to
403 be more affected, because the proportion of the largest patch relative to total forest area (RS_{max}) is near
404 30%, which could indicate that the transition is already started. Moreover, this region was estimated to be
405 potentially bistable, with the possibility to completely transform into a savanna (Staver, Archibald, & Levin,
406 2011). The main driver of deforestation in this area was smallholder farming.

407 The region of South America tropical forest has a RS_{max} of more than 60%, suggesting that the fragmentation
408 transition is approaching but not yet started. In this region, a striking decline in deforestation rates has
409 been observed in Brasil, which hosts most of the biggest forest patch, but deforestation rates have continued
410 to increase in surrounding countries (Argentina, Paraguay, Bolivia, Colombia, Peru) thus the region is still
411 at a high risk.

412 The analysis of RS_{max} reveals that the island of Philippines (SEAS2) seems to be an example of a critical
413 transition from an unconnected to a connected state, the early warning signals can be qualitatively observed:
414 a big fluctuation in a negative direction precedes the transition and then RS_{max} stabilizes over 60% (Figure
415 S9). In addition, there was a total loss of forest cover of 1.9% from year 2000 to 2012 (M. C. Hansen et al.,
416 2013) and deforestation rates were not substantially reduced in 1990-2014; this could be the results of an
417 active intervention of the government promoting conservation and rehabilitation of protected areas, ban of
418 logging old-growth forest, reforestation of barren areas, community-based forestry activities, and sustainable
419 forest management in the country's production forest (Lasco et al., 2008). This confirms that the early
420 warning indicators proposed here work in the correct direction.

421 The region of Southeast Asia was also one of the most deforested places in the world, but was not detected
422 as a region near a fragmentation threshold. This is probably due to the forest conservation and restoration
423 programs implemented by the Chinese government, which bans logging in natural forests and monitor illegal
424 harvesting (Viña, McConnell, Yang, Xu, & Liu, 2016). The MODIS dataset does not detect if native forest
425 is replaced by agroindustrial tree plantations like oil palms, that are among the main drivers of deforestation
426 in this area (Malhi, Gardner, Goldsmith, Silman, & Zelazowski, 2014). To improve the estimation of forest
427 patches, data sets as the MODIS cropland probability and others about land use, protected areas, forest
428 type, should be incorporated (M. Hansen et al., 2014; J. O. Sexton et al., 2015).

429 Deforestation and fragmentation are closely related. At low levels of habitat reduction species population
430 will decline proportionally; this can happen even when the habitat fragments retain connectivity. As habi-
431 tation reduction continues, the critical threshold is approached and connectivity will have large fluctuations
432 (Brook, Ellis, Perring, Mackay, & Blomqvist, 2013). This could trigger several negative synergistic effects:
433 populations fluctuations and the possibility of extinctions will rise, increasing patch isolation and decreasing
434 connectivity (Brook et al., 2013). This positive feedback mechanism will be enhanced when the fragmenta-
435 tion threshold is reached, resulting in the loss of most habitat specialist species at a landscape scale (Pardini
436 et al., 2010). Some authors argue that since species have heterogeneous responses to habitat loss and frag-
437 mentation, and biotic dispersal is limited, the importance of thresholds is restricted to local scales or even
438 that its existence is questionable (Brook et al., 2013). Fragmentation is by definition a local process that at

439 some point produces emergent phenomena over the entire landscape, even if the area considered is infinite
440 (B. Oborny, Meszéna, & Szabó, 2005). In addition, after a region's fragmentation threshold connectivity
441 decreases, there is still a large and internally well connected patch that can maintain sensitive species (A. C.
442 Martensen, Ribeiro, Banks-Leite, Prado, & Metzger, 2012). What is the time needed for these large patches
443 to become fragmented, and pose a real danger of extinction to a myriad of sensitive species? If a forest is
444 already in a fragmented state, a second critical transition from forest to non-forest could happen, this was
445 called the desertification transition (Corrado et al., 2014). Considering the actual trends of habitat loss,
446 and studying the dynamics of non-forest patches—instead of the forest patches as we did here—the risk of
447 this kind of transition could be estimated. The simple models proposed previously could also be used to
448 estimate if these thresholds are likely to be continuous and reversible or discontinuous and often irreversible
449 (Weissmann & Shnerb, 2016), and the degree of protection (e.g. using the set-asides strategy Banks-Leite et
450 al. (2014)) than would be necessary to stop this trend.

451 The effectiveness of landscape management is related to the degree of fragmentation, and the criteria to
452 direct reforestation efforts could be focused on regions near a transition (B. Oborny et al., 2007). Regions
453 that are in an unconnected state require large efforts to recover a connected state, but regions that are near
454 a transition could be easily pushed to a connected state; feedbacks due to facilitation mechanisms might
455 help to maintain this state. Crossing the fragmentation critical point in forests could have negative effects
456 on biodiversity and ecosystem services (Haddad et al., 2015), but it could also produce feedback loops at
457 different levels of the biological hierarchy. This means that a critical transition produced at a continental
458 scale could have effects at the level of communities, food webs, populations, phenotypes and genotypes
459 (Barnosky et al., 2012). All these effects interact with climate change, thus there is a potential production of
460 cascading effects that could lead to a global collapse. Therefore, even if critical thresholds are reached only in
461 some forest regions at a continental scale, a cascading effect with global consequences could still be produced,
462 and may contribute to reach a planetary tipping point (Reyer, Rammig, Brouwers, & Langerwisch, 2015).
463 The risk of such event will be higher if the dynamics of separate continental regions are coupled (Lenton &
464 Williams, 2013). Using the time series obtained in this work the coupling of the continental could be further
465 investigated. It has been proposed that to assess the probability of a global scale shift, different small scale
466 ecosystems should be studied in parallel (Barnosky et al., 2012). As forest comprises a major proportion
467 of such ecosystems, we think that the transition of forests could be used as a proxy for all the underling
468 changes and as a successful predictor of a planetary tipping point.

469 **Supporting information**

470 **Appendix**

471 *Table S1:* Mean power-law exponent and Bootstrapped 95% confidence intervals by threshold.

472 *Table S2:* Mean power-law exponent and Bootstrapped 95% confidence intervals across thresholds by region
473 and year.

474 *Table S3:* Mean total patch area; largest patch S_{max} in km²; largest patch proportional to total patch area
475 RS_{max} and 95% bootstrapped confidence interval of RS_{max} , by region and thresholds, averaged across years

476 *Table S4:* Model selection for distributions of fluctuation of largest patch ΔS_{max} and largest patch relative
477 to total forest area ΔRS_{max} .

478 *Table S5:* Quantil regressions of the fluctuations of the largest patch vs year, for 10% and 90% quantils at
479 different pixel thresholds.

480 *Table S6:* Unbiased estimation of Skewness of fluctuations of the largest patch ΔS_{max} and fluctuations
481 relative to total forest area ΔRS_{max} .

482 *Figure S1:* Regions for Africa: Mainland (AF1), Madagascar (AF2).

483 *Figure S2:* Regions for Eurasia: Mainland (EUAS1), Japan (EUAS2), Great Britain (EUAS3).

484 *Figure S3:* Regions for North America: Mainland (NA1), Newfoundland (NA5).

485 *Figure S4:* Regions for Australia and islands: Australia mainland (OC1), New Guinea (OC2),
486 Malaysia/Kalimantan (OC3), Sumatra (OC4), Sulawesi (OC5), New Zealand south island (OC6),
487 Java (OC7), New Zealand north island (OC8).

488 *Figure S5:* Regions for South America: Tropical and subtropical forest up to Mexico (SAST1), Cuba
489 (SAST2), South America Temperate forest (SAT1).

490 *Figure S6:* Regions for Southeast Asia: Mainland (SEAS1), Philippines (SEAS2).

491 *Figure S7:* Proportion of best models selected for patch size distributions using the Akaike criterion.

492 *Figure S8:* Power law exponents for forest patch distributions by year for all regions.

493 *Figure S9:* Average largest patch relative to total forest area RS_{max} by threshold, for all regions.

494 *Figure S10:* Largest patch relative to total forest area RS_{max} by year at 40% threshold, for regions with
495 total forest area less than 10^7 km².

496 *Figure S11:* Fluctuations of largest patch relative to total forest area RS_{max} for regions with total forest
497 area less than 10^7 km^2 by year and threshold.

498 **Data Accessibility**

499 Csv text file with model fits for patch size distribution, and model selection for all the regions; Gif Animations
500 of a forest model percolation; Gif animations of largest patches; patch size files for all years and regions used
501 here; and all the R, Python and Matlab scripts are available at figshare [http://dx.doi.org/10.6084/m9.
502 figshare.4263905](http://dx.doi.org/10.6084/m9.figshare.4263905).

503 **Acknowledgments**

504 LAS and SRD are grateful to the National University of General Sarmiento for financial support. This work
505 was partially supported by a grant from CONICET (PIO 144-20140100035-CO).

506 **References**

- 507 Allington, G. R. H., & Valone, T. J. (2010). Reversal of desertification: The role of physical and chemical
508 soil properties. *Journal of Arid Environments*, 74(8), 973–977. doi:10.1016/j.jaridenv.2009.12.005
- 509 Alstott, J., Bullmore, E., & Plenz, D. (2014). powerlaw: A Python Package for Analysis of Heavy-Tailed
510 Distributions. *PLOS ONE*, 9(1), e85777. Retrieved from <https://doi.org/10.1371/journal.pone.0085777>
- 511 Banks-Leite, C., Pardini, R., Tambosi, L. R., Pearse, W. D., Bueno, A. A., Bruscagin, R. T., ... Metzger,
512 J. P. (2014). Using ecological thresholds to evaluate the costs and benefits of set-asides in a biodiversity
513 hotspot. *Science*, 345(6200), 1041–1045. doi:10.1126/science.1255768
- 514 Barnosky, A. D., Hadly, E. A., Bascompte, J., Berlow, E. L., Brown, J. H., Fortelius, M., ... Smith, A. B.
515 (2012). Approaching a state shift in Earth’s biosphere. *Nature*, 486(7401), 52–58. doi:10.1038/nature11018
- 516 Bascompte, J., & Solé, R. V. (1996). Habitat fragmentation and extinction thresholds in spatially explicit
517 models. *Journal of Animal Ecology*, 65(4), 465–473. doi:10.2307/5781
- 518 Bazant, M. Z. (2000). Largest cluster in subcritical percolation. *Physical Review E*, 62(2), 1660–1669.
519 Retrieved from <http://link.aps.org/doi/10.1103/PhysRevE.62.1660>
- 520 Belward, A. S. (1996). *The IGBP-DIS Global 1 Km Land Cover Data Set “DISCover”: Proposal and*

- 521 *Implementation Plans : Report of the Land Recover Working Group of IGBP-DIS* (p. 61). IGBP-DIS Office.
- 522 Retrieved from <https://books.google.com.ar/books?id=qixsNAAACAAJ>
- 523 Benedetti-Cecchi, L., Tamburello, L., Maggi, E., & Bulleri, F. (2015). Experimental Perturbations Mod-
- 524 ify the Performance of Early Warning Indicators of Regime Shift. *Current Biology*, 25(14), 1867–1872.
- 525 doi:10.1016/j.cub.2015.05.035
- 526 Bestelmeyer, B. T., Duniway, M. C., James, D. K., Burkett, L. M., & Havstad, K. M. (2013). A test of
- 527 critical thresholds and their indicators in a desertification-prone ecosystem: more resilience than we thought.
- 528 *Ecology Letters*, 16, 339–345. doi:10.1111/ele.12045
- 529 Bestelmeyer, B. T., Ellison, A. M., Fraser, W. R., Gorman, K. B., Holbrook, S. J., Laney, C. M., ... Sharma,
- 530 S. (2011). Analysis of abrupt transitions in ecological systems. *Ecosphere*, 2(12), 129. doi:10.1890/ES11-
- 531 00216.1
- 532 Boettiger, C., & Hastings, A. (2012). Quantifying limits to detection of early warning for critical transitions.
- 533 *Journal of the Royal Society Interface*, 9(75), 2527–2539. doi:10.1098/rsif.2012.0125
- 534 Bonan, G. B. (2008). Forests and Climate Change: forcings, Feedbacks, and the Climate Benefits of Forests.
- 535 *Science*, 320(5882), 1444–1449. doi:10.1126/science.1155121
- 536 Botet, R., & Ploszajczak, M. (2004). Correlations in Finite Systems and Their Universal Scaling Properties.
- 537 In K. Morawetz (Ed.), *Nonequilibrium physics at short time scales: Formation of correlations* (pp. 445–466).
- 538 Berlin Heidelberg: Springer-Verlag.
- 539 Brook, B. W., Ellis, E. C., Perring, M. P., Mackay, A. W., & Blomqvist, L. (2013). Does the terrestrial
- 540 biosphere have planetary tipping points? *Trends in Ecology & Evolution*. doi:10.1016/j.tree.2013.01.016
- 541 Burnham, K., & Anderson, D. R. (2002). *Model selection and multi-model inference: A practical information-*
- 542 *theoretic approach* (2nd. ed., p. 512). New York: Springer-Verlag.
- 543 Canfield, D. E., Glazer, A. N., & Falkowski, P. G. (2010). The Evolution and Future of Earth's Nitrogen
- 544 Cycle. *Science*, 330(6001), 192–196. doi:10.1126/science.1186120
- 545 Carpenter, S. R., Cole, J. J., Pace, M. L., Batt, R., Brock, W. A., Cline, T., ... Weidel, B. (2011).
- 546 Early Warnings of Regime Shifts: A Whole-Ecosystem Experiment. *Science*, 332(6033), 1079–1082.
- 547 doi:10.1126/science.1203672
- 548 Clauset, A., Shalizi, C., & Newman, M. (2009). Power-Law Distributions in Empirical Data. *SIAM Review*,

- 549 51(4), 661–703. doi:10.1137/070710111
- 550 Corrado, R., Cherubini, A. M., & Pennetta, C. (2014). Early warning signals of desertification transitions
551 in semiarid ecosystems. *Physical Review E - Statistical, Nonlinear, and Soft Matter Physics*, 90(6), 62705.
552 doi:10.1103/PhysRevE.90.062705
- 553 Crawley, M. J. (2012). *The R Book* (2nd. ed., p. 1076). Hoboken, NJ, USA: Wiley.
- 554 Crowther, T. W., Glick, H. B., Covey, K. R., Bettigole, C., Maynard, D. S., Thomas, S. M., ... Bradford, M.
555 A. (2015). Mapping tree density at a global scale. *Nature*, 525(7568), 201–205. doi:10.1038/nature14967
- 556 Dai, L., Vorselen, D., Korolev, K. S., & Gore, J. (2012). Generic Indicators for Loss of Resilience Before a
557 Tipping Point Leading to Population Collapse. *Science*, 336(6085), 1175–1177. doi:10.1126/science.1219805
- 558 DiMiceli, C., Carroll, M., Sohlberg, R., Huang, C., Hansen, M., & Townshend, J. (2015). Annual Global Au-
559 tomated MODIS Vegetation Continuous Fields (MOD44B) at 250 m Spatial Resolution for Data Years Begin-
560 ning Day 65, 2000 - 2014, Collection 051 Percent Tree Cover, University of Maryland, College Park, MD, USA.
561 Retrieved from https://lpdaac.usgs.gov/dataset{_}discovery/modis/modis{_}products{_}table/mod44b
- 562 Drake, J. M., & Griffen, B. D. (2010). Early warning signals of extinction in deteriorating environments.
563 *Nature*, 467(7314), 456–459. doi:10.1038/nature09389
- 564 Efron, B., & Tibshirani, R. J. (1994). *An Introduction to the Bootstrap* (p. 456). New York: Taylor &
565 Francis. Retrieved from <https://books.google.es/books?id=gLlpIUXRntoC>
- 566 Filotas, E., Parrott, L., Burton, P. J., Chazdon, R. L., Coates, K. D., Coll, L., ... Messier, C. (2014). Viewing
567 forests through the lens of complex systems science. *Ecosphere*, 5(January), 1–23. doi:10.1890/ES13-00182.1
- 568 Foley, J. A., Ramankutty, N., Brauman, K. A., Cassidy, E. S., Gerber, J. S., Johnston, M., ... Zaks, D. P. M.
569 (2011). Solutions for a cultivated planet. *Nature*, 478(7369), 337–342. doi:10.1038/nature10452
- 570 Folke, C., Jansson, Å., Rockström, J., Olsson, P., Carpenter, S. R., Iii, F. S. C., ... Westley, F. (2011).
571 Reconnecting to the Biosphere. *AMBIO*, 40(7), 719–738. doi:10.1007/s13280-011-0184-y
- 572 Fung, T., O'Dwyer, J. P., Rahman, K. A., Fletcher, C. D., & Chisholm, R. A. (2016). Reproducing static
573 and dynamic biodiversity patterns in tropical forests: the critical role of environmental variance. *Ecology*,
574 97(5), 1207–1217. doi:10.1890/15-0984.1
- 575 Gardner, R. H., & Urban, D. L. (2007). Neutral models for testing landscape hypotheses. *Landscape Ecology*,
576 22(1), 15–29. doi:10.1007/s10980-006-9011-4
- 577 Gastner, M. T., Oborny, B., Zimmermann, D. K., & Pruessner, G. (2009). Transition from Connected

- 578 to Fragmented Vegetation across an Environmental Gradient: Scaling Laws in Ecotone Geometry. *The*
579 *American Naturalist*, 174(1), E23–E39. doi:10.1086/599292
- 580 Gilman, S. E., Urban, M. C., Tewksbury, J., Gilchrist, G. W., & Holt, R. D. (2010). A framework
581 for community interactions under climate change. *Trends in Ecology & Evolution*, 25(6), 325–331.
582 doi:10.1016/j.tree.2010.03.002
- 583 Goldstein, M. L., Morris, S. A., & Yen, G. G. (2004). Problems with fitting to the power-law distri-
584 bution. *The European Physical Journal B - Condensed Matter and Complex Systems*, 41(2), 255–258.
585 doi:10.1140/epjb/e2004-00316-5
- 586 Haddad, N. M., Brudvig, L. a., Clobert, J., Davies, K. F., Gonzalez, A., Holt, R. D., ... Townshend, J. R.
587 (2015). Habitat fragmentation and its lasting impact on Earth's ecosystems. *Science Advances*, 1(2), 1–9.
588 doi:10.1126/sciadv.1500052
- 589 Hansen, M. C., Potapov, P. V., Moore, R., Hancher, M., Turubanova, S. A., Tyukavina, A., ... Townshend,
590 J. R. G. (2013). High-Resolution Global Maps of 21st-Century Forest Cover Change. *Science*, 342(6160),
591 850–853. doi:10.1126/science.1244693
- 592 Hansen, M., Potapov, P., Margono, B., Stehman, S., Turubanova, S., & Tyukavina, A. (2014). Response
593 to Comment on “High-resolution global maps of 21st-century forest cover change”. *Science*, 344(6187), 981.
594 doi:10.1126/science.1248817
- 595 Hantson, S., Pueyo, S., & Chuvieco, E. (2015). Global fire size distribution is driven by human impact and
596 climate. *Global Ecology and Biogeography*, 24(1), 77–86. doi:10.1111/geb.12246
- 597 Harris, T. E. (1974). Contact interactions on a lattice. *The Annals of Probability*, 2, 969–988.
- 598 Hartigan, J. A., & Hartigan, P. M. (1985). The Dip Test of Unimodality. *The Annals of Statistics*, 13(1),
599 70–84. Retrieved from <http://www.jstor.org/stable/2241144>
- 600 Hastings, A., & Wysham, D. B. (2010). Regime shifts in ecological systems can occur with no warning.
601 *Ecology Letters*, 13(4), 464–472. doi:10.1111/j.1461-0248.2010.01439.x
- 602 He, F., & Hubbell, S. (2003). Percolation Theory for the Distribution and Abundance of Species. *Physical*
603 *Review Letters*, 91(19), 198103. doi:10.1103/PhysRevLett.91.198103
- 604 Hinrichsen, H. (2000). Non-equilibrium critical phenomena and phase transitions into absorbing states.
605 *Advances in Physics*, 49(7), 815–958. doi:10.1080/00018730050198152
- 606 Hirota, M., Holmgren, M., Nes, E. H. V., & Scheffer, M. (2011). Global Resilience of Tropical Forest and

- 607 Savanna to Critical Transitions. *Science*, 334(6053), 232–235. doi:10.1126/science.1210657
- 608 Irvine, M. A., Bull, J. C., & Keeling, M. J. (2016). Aggregation dynamics explain vegetation patch-size
609 distributions. *Theoretical Population Biology*, 108, 70–74. doi:10.1016/j.tpb.2015.12.001
- 610 Keitt, T. H., Urban, D. L., & Milne, B. T. (1997). Detecting critical scales in fragmented landscapes.
611 *Conservation Ecology*, 1(1), 4. Retrieved from <http://www.ecologyandsociety.org/vol1/iss1/art4/>
- 612 Kéfi, S., Guttal, V., Brock, W. A., Carpenter, S. R., Ellison, A. M., Livina, V. N., ... Dakos, V. (2014).
613 Early Warning Signals of Ecological Transitions: Methods for Spatial Patterns. *PLoS ONE*, 9(3), e92097.
614 doi:10.1371/journal.pone.0092097
- 615 Kéfi, S., Rietkerk, M., Alados, C. L., Pueyo, Y., Papanastasis, V. P., ElAich, A., & Ruiter, P. C. de.
616 (2007). Spatial vegetation patterns and imminent desertification in Mediterranean arid ecosystems. *Nature*,
617 449(7159), 213–217. doi:10.1038/nature06111
- 618 Kitzberger, T., Aráoz, E., Gowda, J. H., Mermoz, M., & Morales, J. M. (2012). Decreases in Fire Spread
619 Probability with Forest Age Promotes Alternative Community States, Reduced Resilience to Climate Vari-
620 ability and Large Fire Regime Shifts. *Ecosystems*, 15(1), 97–112. doi:10.1007/s10021-011-9494-y
- 621 Koenker, R. (2016). quantreg: Quantile Regression. Retrieved from <http://cran.r-project.org/package=quantreg>
- 622
- 623 Lasco, R. D., Pulhin, F. B., Cruz, R. V. O., Pulhin, J. M., Roy, S. S. N., & Sanchez, P. A. J. (2008). Forest
624 responses to changing rainfall in the Philippines. In N. Leary, C. Conde, & J. Kulkarni (Eds.), *Climate
625 change and vulnerability* (pp. 49–66). London: Earthscan. Retrieved from <http://gen.lib.rus.ec/book/index.php?md5=AD313B13E05C9D61A9EC1EE2E73A91FB>
- 626
- 627 Leibold, M. A., & Norberg, J. (2004). Biodiversity in metacommunities: Plankton as complex adaptive
628 systems? *Limnology and Oceanography*, 49(4, part 2), 1278–1289. doi:10.4319/lo.2004.49.4_part_2.1278
- 629 Lenton, T. M., & Williams, H. T. P. (2013). On the origin of planetary-scale tipping points. *Trends in
630 Ecology & Evolution*, 28(7), 380–382. doi:10.1016/j.tree.2013.06.001
- 631 Limpert, E., Stahel, W. A., & Abbt, M. (2001). Log-normal Distributions across the Sciences: Keys and
632 CluesOn the charms of statistics, and how mechanical models resembling gambling machines offer a link to
633 a handy way to characterize log-normal distributions, which can provide deeper insight into var. *BioScience*,
634 51(5), 341–352. Retrieved from [http://dx.doi.org/10.1641/0006-3568\(2001\)051\[0341:LNDATS\]2.0.CO](http://dx.doi.org/10.1641/0006-3568(2001)051[0341:LNDATS]2.0.CO)
- 635 Loehle, C., Li, B.-L., & Sundell, R. C. (1996). Forest spread and phase transitions at forest-prairie ecotones

- 636 in Kansas, U.S.A. *Landscape Ecology*, 11(4), 225–235.
- 637 Malhi, Y., Gardner, T. A., Goldsmith, G. R., Silman, M. R., & Zelazowski, P. (2014). Tropical Forests in
638 the Anthropocene. *Annual Review of Environment and Resources*, 39(1), 125–159. doi:10.1146/annurev-
639 environ-030713-155141
- 640 Manor, A., & Shnerb, N. M. (2008). Origin of pareto-like spatial distributions in ecosystems. *Physical*
641 *Review Letters*, 101(26), 268104. doi:10.1103/PhysRevLett.101.268104
- 642 Martensen, A. C., Ribeiro, M. C., Banks-Leite, C., Prado, P. I., & Metzger, J. P. (2012). Associations
643 of Forest Cover, Fragment Area, and Connectivity with Neotropical Understory Bird Species Richness and
644 Abundance. *Conservation Biology*, 26(6), 1100–1111. doi:10.1111/j.1523-1739.2012.01940.x
- 645 McKenzie, D., & Kennedy, M. C. (2012). Power laws reveal phase transitions in landscape con-
646 trols of fire regimes. *Nat Commun*, 3, 726. Retrieved from <http://dx.doi.org/10.1038/ncomms1731>
647 http://www.nature.com/ncomms/journal/v3/n3/suppinfo/ncomms1731{__}S1.html
- 648 Mitchell, M. G. E., Suarez-Castro, A. F., Martinez-Harms, M., Maron, M., McAlpine, C., Gaston, K. J., ...
649 Rhodes, J. R. (2015). Reframing landscape fragmentation's effects on ecosystem services. *Trends in Ecology*
650 & Evolution, 30(4), 190–198. doi:10.1016/j.tree.2015.01.011
- 651 Naito, A. T., & Cairns, D. M. (2015). Patterns of shrub expansion in Alaskan arctic river corridors suggest
652 phase transition. *Ecology and Evolution*, 5(1), 87–101. doi:10.1002/ece3.1341
- 653 Newman, M. E. J. (2005). Power laws, Pareto distributions and Zipf's law. *Contemporary Physics*, 46(5),
654 323–351. doi:10.1080/00107510500052444
- 655 Oborny, B., Meszéna, G., & Szabó, G. (2005). Dynamics of Populations on the Verge of Extinction. *Oikos*,
656 109(2), 291–296. Retrieved from <http://www.jstor.org/stable/3548746>
- 657 Oborny, B., Szabó, G., & Meszéna, G. (2007). Survival of species in patchy landscapes: percolation in
658 space and time. In *Scaling biodiversity* (pp. 409–440). Cambridge University Press. Retrieved from <http://dx.doi.org/10.1017/CBO9780511814938.022>
- 660 Ochoa-Quintero, J. M., Gardner, T. A., Rosa, I., de Barros Ferraz, S. F., & Sutherland, W. J. (2015).
661 Thresholds of species loss in Amazonian deforestation frontier landscapes. *Conservation Biology*, 29(2),
662 440–451. doi:10.1111/cobi.12446
- 663 Ódor, G. (2004). Universality classes in nonequilibrium lattice systems. *Reviews of Modern Physics*, 76(3)

- 664 I), 663–724. doi:10.1103/RevModPhys.76.663
- 665 Pardini, R., Bueno, A. de A., Gardner, T. A., Prado, P. I., & Metzger, J. P. (2010). Beyond the Fragmen-
666 tation Threshold Hypothesis: Regime Shifts in Biodiversity Across Fragmented Landscapes. *PLoS ONE*,
667 5(10), e13666. doi:10.1371/journal.pone.0013666
- 668 Potapov, P., Yaroshenko, A., Turubanova, S., Dubinin, M., Laestadius, L., Thies, C., ... Zhuravleva, I. (2008).
669 Mapping the world's intact forest landscapes by remote sensing. *Ecology and Society*, 13(2).
- 670 Pueyo, S., de Alencastro Graça, P. M. L., Barbosa, R. I., Cots, R., Cardona, E., & Fearnside, P. M. (2010).
671 Testing for criticality in ecosystem dynamics: the case of Amazonian rainforest and savanna fire. *Ecology
Letters*, 13(7), 793–802. doi:10.1111/j.1461-0248.2010.01497.x
- 672 673 R Core Team. (2015). R: A Language and Environment for Statistical Computing. Vienna, Austria: R
674 Foundation for Statistical Computing. Retrieved from <http://www.r-project.org/>
- 675 Reyer, C. P. O., Rammig, A., Brouwers, N., & Langerwisch, F. (2015). Forest resilience, tipping points and
676 global change processes. *Journal of Ecology*, 103(1), 1–4. doi:10.1111/1365-2745.12342
- 677 Rockstrom, J., Steffen, W., Noone, K., Persson, A., Chapin, F. S., Lambin, E. F., ... Foley, J. A. (2009). A
678 safe operating space for humanity. *Nature*, 461(7263), 472–475. Retrieved from [http://dx.doi.org/10.1038/461472a](http://dx.doi.org/10.1038/
679 461472a)
- 680 Rooij, M. M. J. W. van, Nash, B., Rajaraman, S., & Holden, J. G. (2013). A Fractal Approach to Dynamic
681 Inference and Distribution Analysis. *Frontiers in Physiology*, 4(1). doi:10.3389/fphys.2013.00001
- 682 Saravia, L. A., & Momo, F. R. (2017). Biodiversity collapse and early warning indicators in
683 a spatial phase transition between neutral and niche communities. *PeerJ PrePrints*, 5, e1589v4.
684 doi:10.7287/peerj.preprints.1589v3
- 685 Scanlon, T. M., Caylor, K. K., Levin, S. A., & Rodriguez-iturbe, I. (2007). Positive feedbacks promote
686 power-law clustering of Kalahari vegetation. *Nature*, 449(September), 209–212. doi:10.1038/nature06060
- 687 Scheffer, M., Bascompte, J., Brock, W. A., Brovkin, V., Carpenter, S. R., Dakos, V., ... Sugihara, G. (2009).
688 Early-warning signals for critical transitions. *Nature*, 461(7260), 53–59. doi:10.1038/nature08227
- 689 Scheffer, M., Walker, B., Carpenter, S., Foley, J. a, Folke, C., & Walker, B. (2001). Catastrophic shifts in
690 ecosystems. *Nature*, 413(6856), 591–596. doi:10.1038/35098000
- 691 Seidler, T. G., & Plotkin, J. B. (2006). Seed Dispersal and Spatial Pattern in Tropical Trees. *PLoS Biology*,

- 692 4(11), e344. doi:10.1371/journal.pbio.0040344
- 693 Sexton, J. O., Noojipady, P., Song, X.-P., Feng, M., Song, D.-X., Kim, D.-H., ... Townshend, J. R.
694 (2015). Conservation policy and the measurement of forests. *Nature Climate Change*, 6(2), 192–196.
695 doi:10.1038/nclimate2816
- 696 Sexton, J. O., Song, X.-P., Feng, M., Noojipady, P., Anand, A., Huang, C., ... Townshend, J. R. (2013).
697 Global, 30-m resolution continuous fields of tree cover: Landsat-based rescaling of MODIS vegetation con-
698 tinuous fields with lidar-based estimates of error. *International Journal of Digital Earth*, 6(5), 427–448.
699 doi:10.1080/17538947.2013.786146
- 700 Solé, R. V. (2011). *Phase Transitions* (p. 223). Princeton University Press. Retrieved from <https://books.google.com.ar/books?id=8RcLuv-Ll2kC>
- 702 Solé, R. V., & Bascompte, J. (2006). *Self-organization in complex ecosystems* (p. 373). New Jersey, USA.:
703 Princeton University Press. Retrieved from <http://books.google.com.ar/books?id=v4gpGH6Gv68C>
- 704 Solé, R. V., Alonso, D., & Mckane, A. (2002). Self-organized instability in complex ecosystems. *Philoso-
705 sophical Transactions of the Royal Society of London. Series B, Biological Sciences*, 357(May), 667–681.
706 doi:10.1098/rstb.2001.0992
- 707 Solé, R. V., Alonso, D., & Saldaña, J. (2004). Habitat fragmentation and biodiversity collapse in neutral
708 communities. *Ecological Complexity*, 1(1), 65–75. doi:10.1016/j.ecocom.2003.12.003
- 709 Solé, R. V., Bartumeus, F., & Gamarra, J. G. P. (2005). Gap percolation in rainforests. *Oikos*, 110(1),
710 177–185. doi:10.1111/j.0030-1299.2005.13843.x
- 711 Staal, A., Dekker, S. C., Xu, C., & Nes, E. H. van. (2016). Bistability, Spatial Interaction, and the
712 Distribution of Tropical Forests and Savannas. *Ecosystems*, 19(6), 1080–1091. doi:10.1007/s10021-016-0011-
713 1
- 714 Stauffer, D., & Aharony, A. (1994). *Introduction To Percolation Theory* (p. 179). London: Taylor & Francis.
- 715 Staver, A. C., Archibald, S., & Levin, S. A. (2011). The Global Extent and Determinants of Savanna and
716 Forest as Alternative Biome States. *Science*, 334(6053), 230–232. doi:10.1126/science.1210465
- 717 Vasilakopoulos, P., & Marshall, C. T. (2015). Resilience and tipping points of an exploited fish population
718 over six decades. *Global Change Biology*, 21(5), 1834–1847. doi:10.1111/gcb.12845
- 719 Verbesselt, J., Umlauf, N., Hirota, M., Holmgren, M., Van Nes, E. H., Herold, M., ... Scheffer, M. (2016). Re-

- 720 motely sensed resilience of tropical forests. *Nature Climate Change*, 1(September). doi:10.1038/nclimate3108
- 721 Villa Martín, P., Bonachela, J. A., & Muñoz, M. A. (2014). Quenched disorder forbids discontinuous
722 transitions in nonequilibrium low-dimensional systems. *Physical Review E*, 89(1), 12145. Retrieved from
723 <https://link.aps.org/doi/10.1103/PhysRevE.89.012145>
- 724 Villa Martín, P., Bonachela, J. A., Levin, S. A., & Muñoz, M. A. (2015). Eluding catastrophic shifts.
725 *Proceedings of the National Academy of Sciences*, 112(15), E1828–E1836. doi:10.1073/pnas.1414708112
- 726 Viña, A., McConnell, W. J., Yang, H., Xu, Z., & Liu, J. (2016). Effects of conservation policy on China's
727 forest recovery. *Science Advances*, 2(3), e1500965. Retrieved from <http://advances.sciencemag.org/content/2/3/e1500965.abstract>
- 729 Vuong, Q. H. (1989). Likelihood Ratio Tests for Model Selection and Non-Nested Hypotheses. *Econometrica*,
730 57(2), 307–333. doi:10.2307/1912557
- 731 Weerman, E. J., Van Belzen, J., Rietkerk, M., Temmerman, S., Kéfi, S., Herman, P. M. J., & Koppell, J. V.
732 de. (2012). Changes in diatom patch-size distribution and degradation in a spatially self-organized intertidal
733 mudflat ecosystem. *Ecology*, 93(3), 608–618. doi:10.1890/11-0625.1
- 734 Weissmann, H., & Shnerb, N. M. (2016). Predicting catastrophic shifts. *Journal of Theoretical Biology*, 397,
735 128–134. doi:10.1016/j.jtbi.2016.02.033
- 736 Wuyts, B., Champneys, A. R., & House, J. I. (2017). Amazonian forest-savanna bistability and human
737 impact. *Nature Communications*, 8(May), 15519. doi:10.1038/ncomms15519
- 738 Xu, C., Hantson, S., Holmgren, M., Nes, E. H. van, Staal, A., & Scheffer, M. (2016). Remotely sensed
739 canopy height reveals three pantropical ecosystem states. *Ecology*, 97(9), 2518–2521. doi:10.1002/ecy.1470
- 740 Zhang, J. Y., Wang, Y., Zhao, X., Xie, G., & Zhang, T. (2005). Grassland recovery by protection from
741 grazing in a semi-arid sandy region of northern China. *New Zealand Journal of Agricultural Research*, 48(2),
742 277–284. doi:10.1080/00288233.2005.9513657
- 743 Zinck, R. D., & Grimm, V. (2009). Unifying wildfire models from ecology and statistical physics. *The
744 American Naturalist*, 174(5), E170–85. doi:10.1086/605959